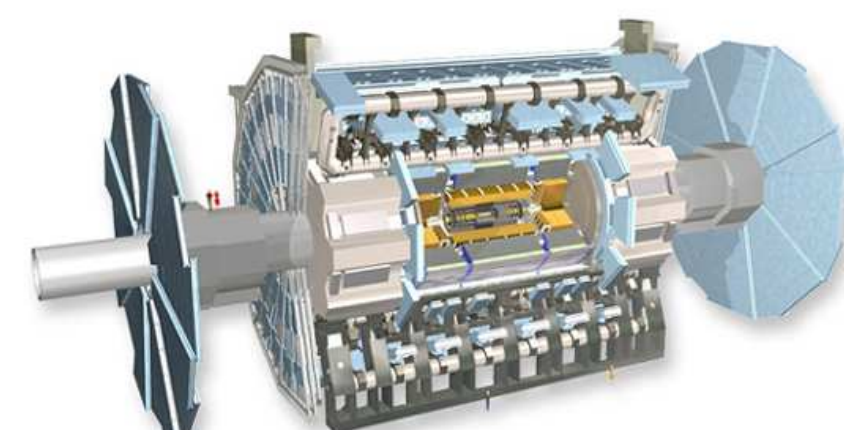




MONITORING OF THE ATLAS LIQUID ARGON CALORIMETER

J.J. Goodson on behalf of the ATLAS Liquid Argon Group
SUNY-Stony Brook, New York, USA



Abstract

The ATLAS detector at the Large Hadron Collider is expected to collect an unprecedented wealth of new data at a completely new energy scale. In particular its Liquid Argon electromagnetic and hadronic calorimeters will play an essential role in measuring final states with electrons and photons and in contributing to the measurement of jets and missing transverse energy. Efficient monitoring of data will be crucial from the earliest data taking and will be implemented at the performance of each sub-detector and their impact on physics quantities, the monitoring will be crucial in guaranteeing data to be ready for physics analysis. The tools and criteria for monitoring the LAr data in the coming data taking will be discussed. The software developed for the monitoring of collision data will be described and results of monitoring performance for data obtained from a full simulation of the data processing that includes data streams foreseen in the ATLAS operation will be presented. The status of automated data quality checks will be shown.

Liquid Argon Calorimeter and Its Systems

The ATLAS Liquid Argon (LAr) calorimeter is one of two detectors used for calorimetry in the ATLAS experiment. Due to the radiation-resistance of a noble gas system, the LAr Calorimeter is used for EM measurements, forward calorimetry, and also for the hadronic measurements in the endcap regions [1]. In the EM sections, the LAr calorimeter is notable for a unique accordion geometry (Fig. 1) that aids hermetic coverage by minimizing cracks. In the hadronic endcaps a more traditional plate geometry is used (Fig. 2). In the forward calorimeters the electrodes form narrow, cylindrical channels filled with liquid argon around electrode cores (see Fig. 3), which reduces ion drift time [1, 2, 3]. The LAr calorimeter in total has 182,000 channels to be read, which a collision frequency of 40 MHz, posing a considerable challenge to monitoring, read-out, and data storage [3].

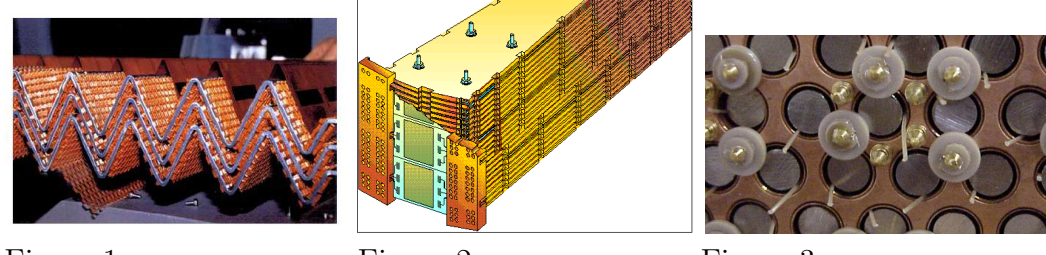


Figure 1

Figure 2

Figure 3

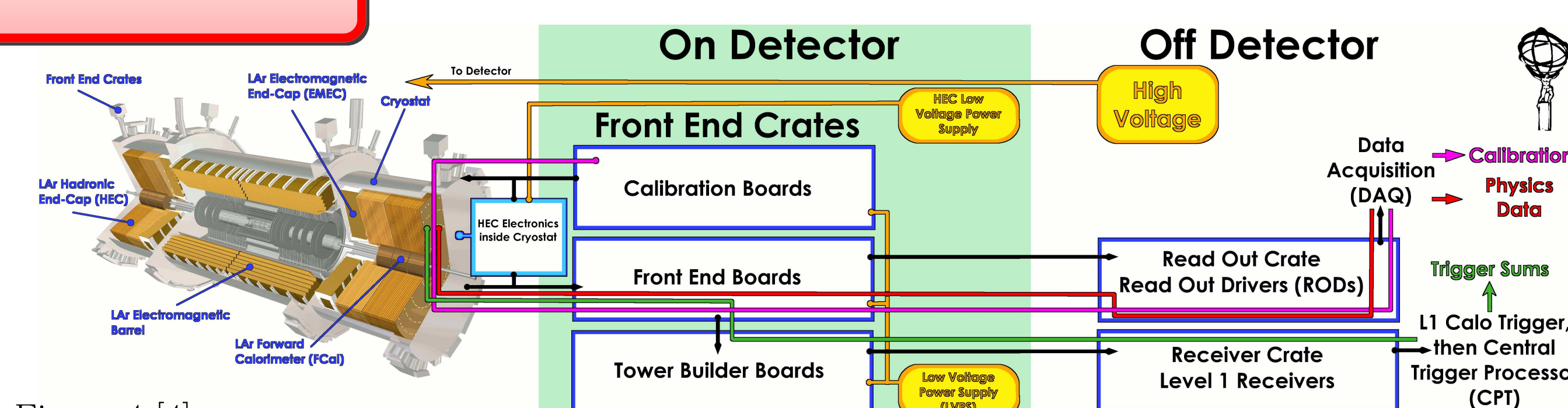


Figure 4 [4]

Calibration Boards

- Uses pulsed to inject current mimicking physics signal
- Used to calculate gain in each channel [3].

Front-End Boards (FEBs)

- Receive analog signals from detector electrodes, then amplifies and shapes the signals.
- Sums cells of the calorimeter into trigger towers of $\Delta\eta \times \Delta\phi = 0.1 \times 0.1$ by layer and prepares Trigger Tower Board input.
- Stores signals in memory until Level-1 trigger decision.
- Digitizes the signals and passes them to Read-Out Drivers and Trigger Builder Boards [5].

Trigger Towers

- In the EM segment the Tower Builder Boards finish the analog sums to make trigger towers and transmit the signal to the Level-1 off-detector electronics for digitization.
- In the Hadronic End Cap, the Tower Builder Boards produce differential signals and pass it on to Level 1 [5].

Read-Out Drivers (RODs)

- Receives the digital signal from the FEBs.
- Computes the energy for each channel, as well as the timing and pulse shape quality measurement (χ^2).
- Monitors raw data and calorimeter parameters, such as temperatures and busy signals.
- Passes data on to Level-2 trigger [5, 6, 3].
- Triangular physics signal reshaped by electronics
- Physics running uses 5 samples, calibration mode uses 32
- Energy computed in Digital Signal Processor, based on amplitude of shaped pulse
- Shaped pulse sampled every 25 ns.

Figure 5 [2]

Trigger and Data Acquisition (TDAQ)

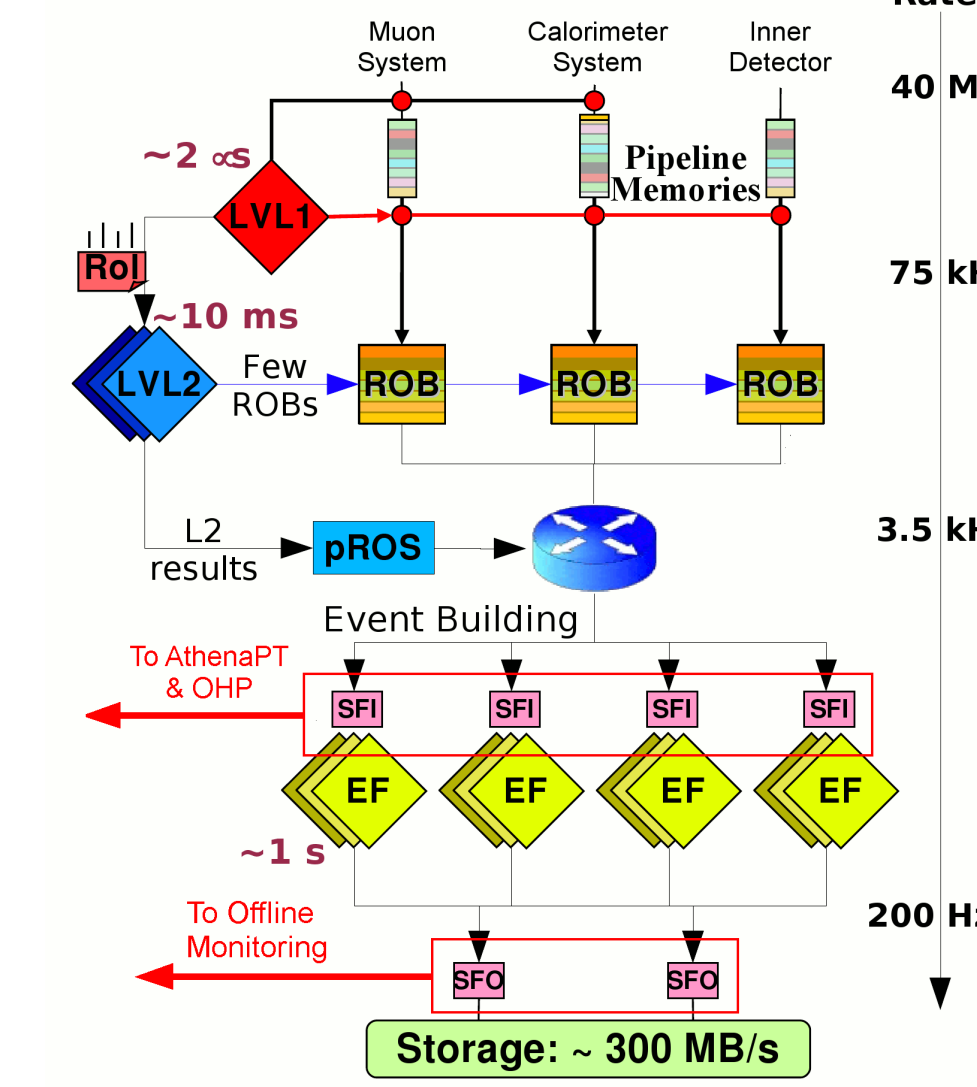


Figure 6 [7, 8]
ROB = Read-Out Buffer (input stage), pROB = pseudo-Read-Out System, SFI = Sub-Farm Input, EF = Event Filter, SFO = Sub-Farm Output

Control Room



Figure 7

Source: Adam Yurkiewicz at BNL, USLHC/LNS

At present the Liquid Argon group keeps 3 shifts on duty for 3 shifts a day during operational periods. The shifters watch for alerts from the detector, or from warnings from other desks in the ATLAS Control, such as Data Quality, Detector Control Systems, or Run Control. They monitor the data coming from the detector which may reveal problems, such as missing subcomponents or noisy cells. In addition, they act as the first stage of offline monitoring, examining data from the initial processing of runs prior to their shift. They also configure the LAr calorimeter for different types of running and take calibration runs.

Detector Control System

The LAr Calorimeter makes use of the same DCS as the rest of the ATLAS experiment. The DCS system allows monitoring of the sub-detector hardware and infrastructure, controls the operation state of the detector, and allows for action to be taken in response to abnormal behavior. The DCS software makes use of the Supervisory Control and Data Acquisition system PVSS from Siemens subsidiary ETM [9].

Figure 9
The DCS panel allows for monitoring of the state of each subsystem, as well as changing the state and turning subcomponents on and off. For each component important values, such as temperature, current, and voltage, can be displayed and their trends plotted.

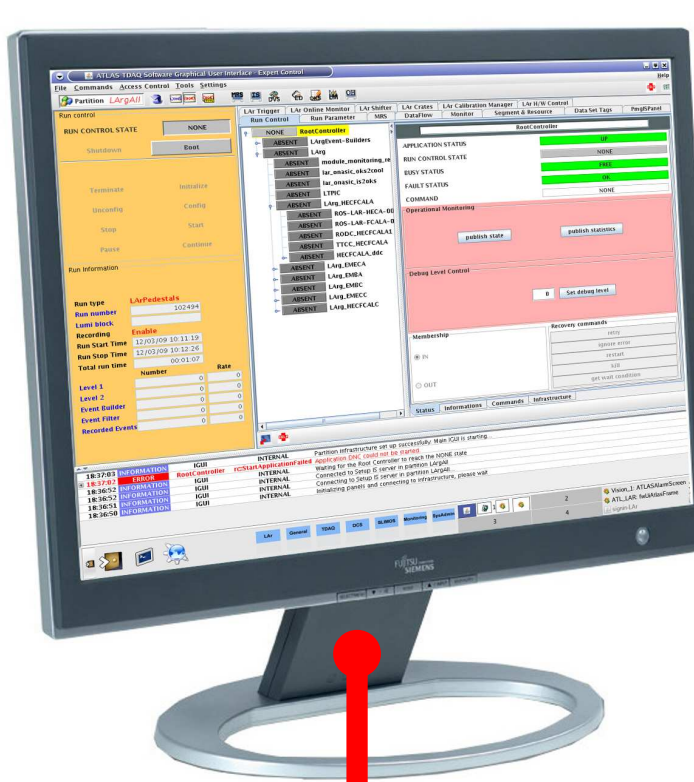


Figure 8
The front-end GUI of the ATLAS TDAQ. Monitoring of the readout of ATLAS and its subdetectors centers on this application, which provides general run information (duration, run number) is displayed, in addition to various software alarms and detector settings. During full detector running a shifter at the LAr station may only monitor through the GUI, but the GUI is also used to manage LAr Calorimeter calibration runs.

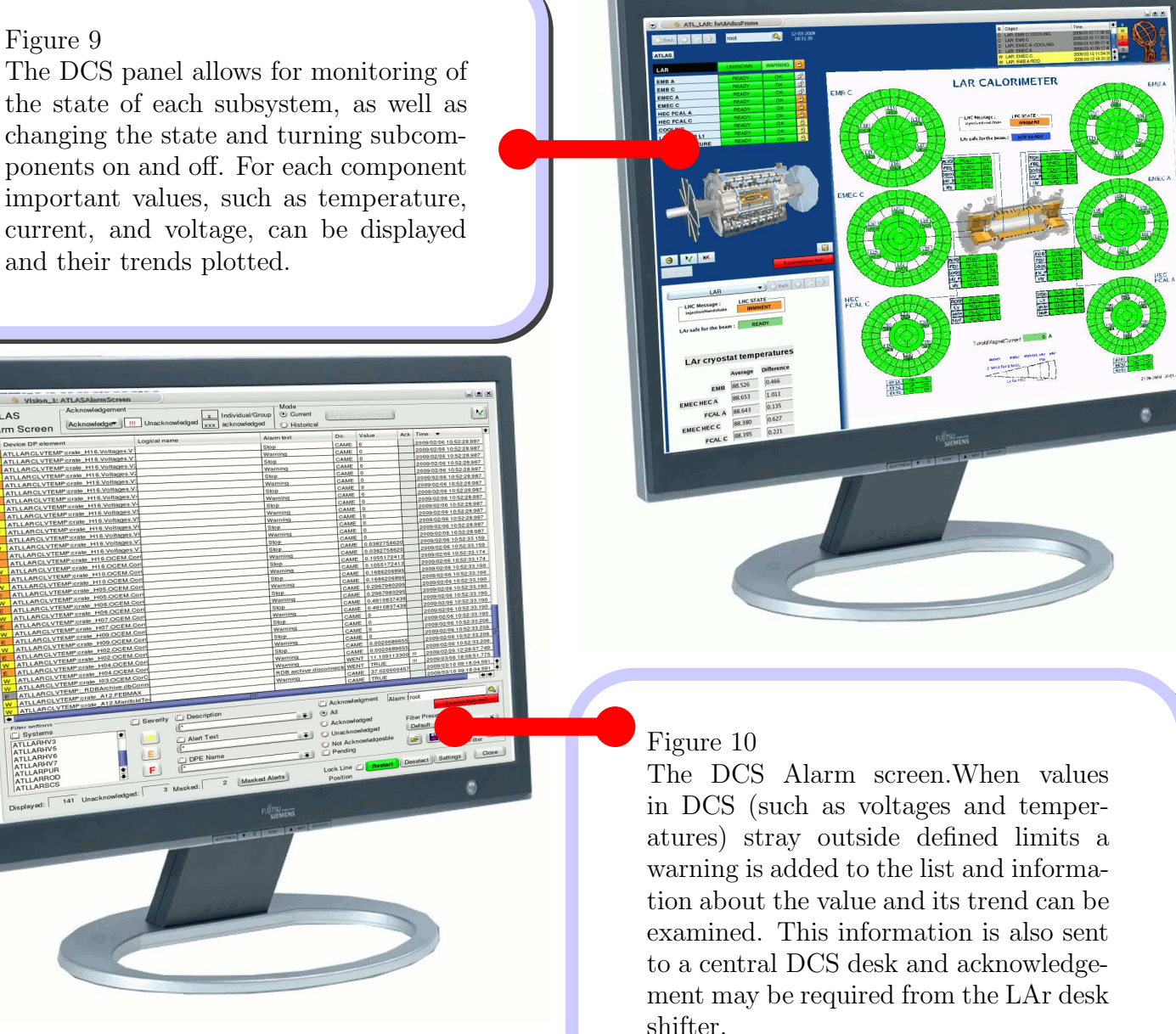


Figure 10
The DCS Alarm screen. When values in DCS (such as voltages and temperatures) stray outside defined limits a warning is added to the list and information about the value and its trend can be examined. This information is also sent to a central DCS desk and acknowledgment may be required from the LAr desk shifter.

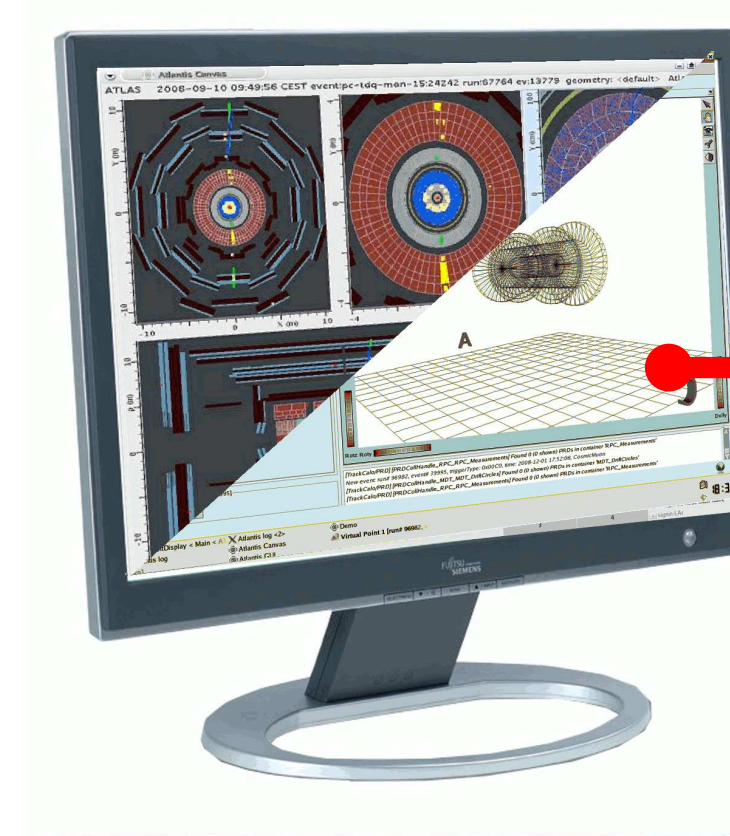


Figure 11
The ATLANTIS event display (top left) is a JAVA based application that presents read-out information mapped to a simplified detector geometry. Used in commissioning, monitoring, and physics analysis. Useful for identifying problem areas in detectors [10].

Virtual Point 1 (bottom right) is an event display integrated into the ATLAS data processing framework used by ATLAS, giving it direct access to the GEANT4 models used in physics analysis and updated with alignment measures and calibrations [11].

Figure 12
The Online Histogram Service is responsible for directing the flow of histograms from all sub-detectors and their component systems and storing them. The Online Histogram Presenter is the universal method for viewing monitoring histograms in ATLAS. The frontend is a GUI based on Trolltech Inc's Qt provides a universal and organized way for LAr shifters to look at the monitoring data coming from the detector [12].

The data is fed to OHP from ATHENA Processing Tasks running in control room computers, using the same framework as physics analysis. The plots monitored include detector coverage, the event frequency, errors in the component systems and the error type, noise, and the output of the ROD DSPs, energy, timing, and quality.

These same plots are also monitored by shifters for runs that have already begun offline processing using dedicated data quality pages or using the ROOT libraries. Important features of the data are logged for future use in calibration and further monitoring.

Offline

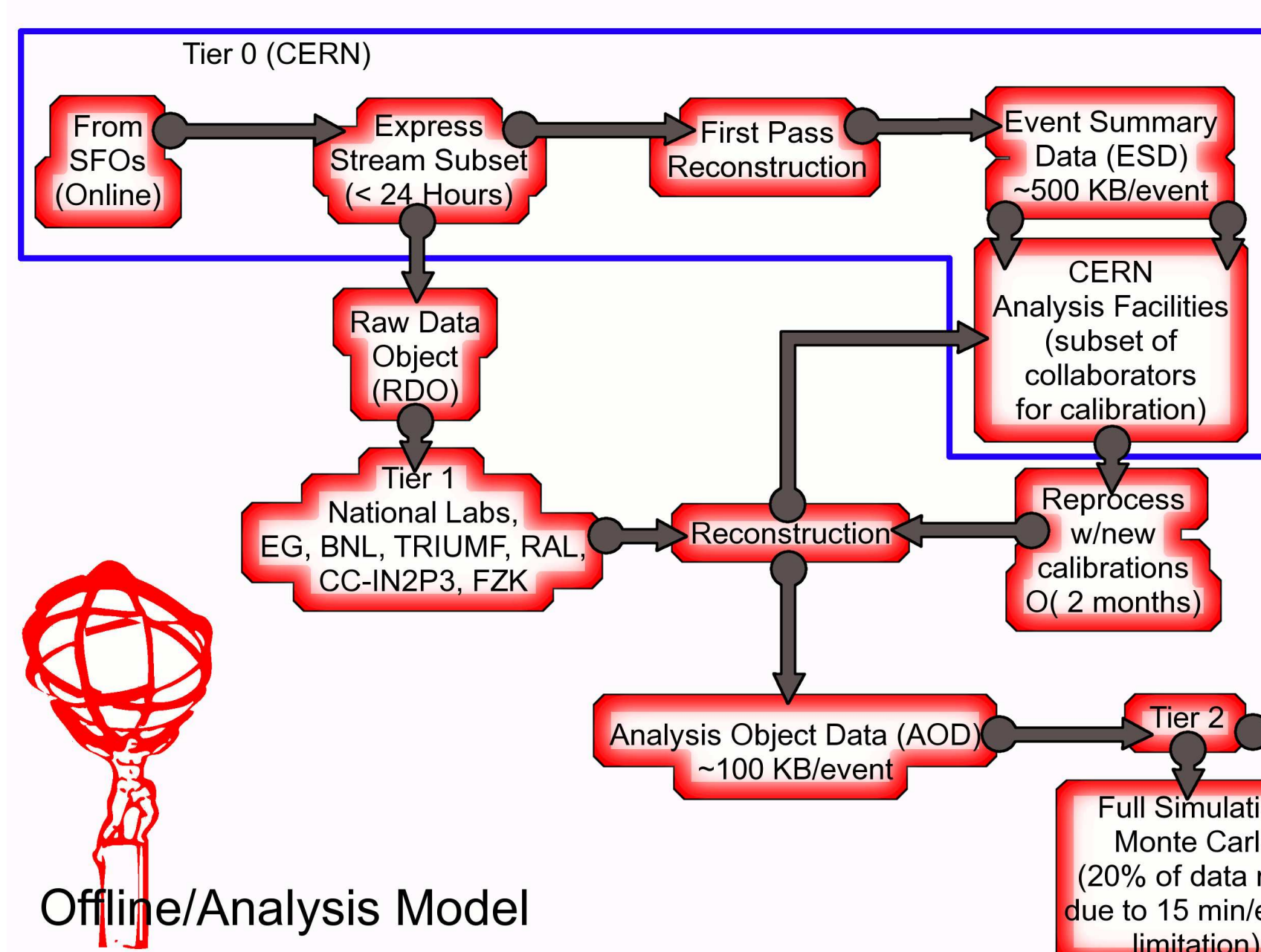


Figure 13 [13]

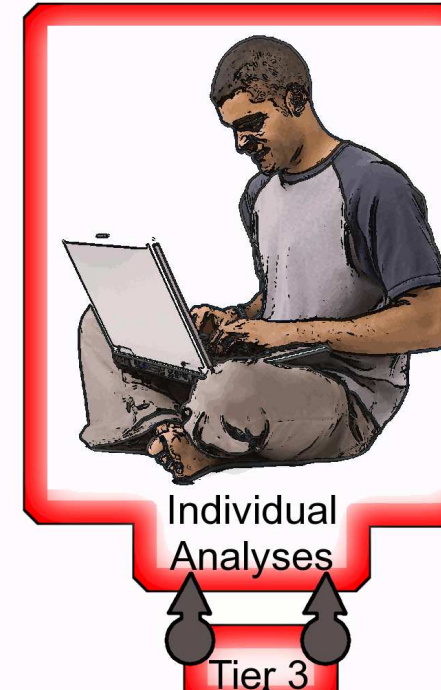


Figure 14
While final bulk processing may take on the order of months to be completed, the initial express stream is immediately available and used by the LAr calorimeter for offline monitoring. Offline monitoring makes use of the same tools used in the control room for online monitoring and examines the same quantities, forming a continuous chain from initial data taking to the end-users analysis based on the ATHENA analysis framework, a derivative of LHCb's Gaudi framework. Offline monitoring is of course more detailed and in depth due to the extended time available over a control room shift.

- High energy digits (samplings of the physics pulse shape)
- Data Integrity/Quality such as coverage dropouts or electronics errors.
- Misbehaving channels, noise and occupancy in cells



Figure 15
The Data Quality web display is used both by LAr shifters online and offline and also by a dedicated Data Quality desk in the control room. Data is flagged based on usability for future analyses and for additional examinations of its usability later in the offline processing.

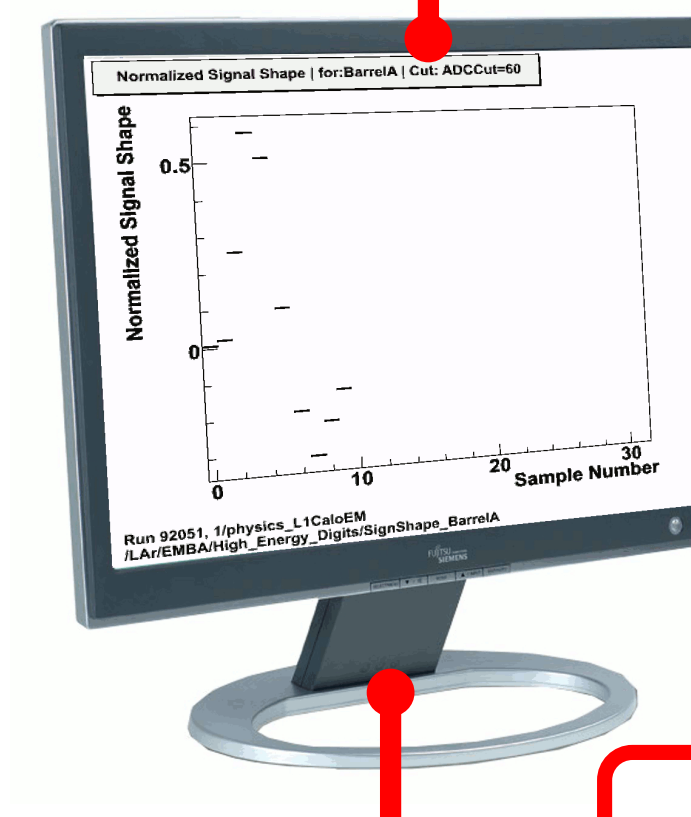


Figure 16
An example of one of the plots used in monitoring: a 10-sample reconstructed pulse (see Fig. 5) from 202,910 events in one half of the EM barrel. A primary usage of this reconstruction is to tune the timing of the LAr calorimeter in order to accurately capture the pulse peak for physics running.

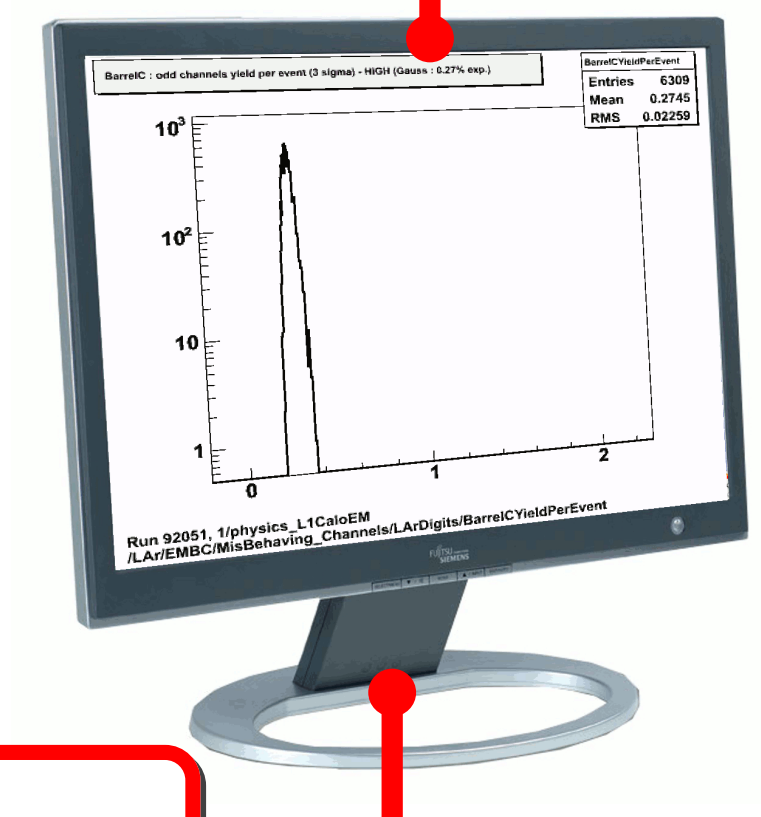


Figure 17
An example of one of the plots used in monitoring: the percent of LAr cells with energies more than 3σ above the reference pedestal/noise, averaged over 6309 events. Assuming Gaussian behavior and a stable pedestal/noise, we expect a peak centered at 0.27%, in general agreement with what we see here.

Cosmic Muon Data Results

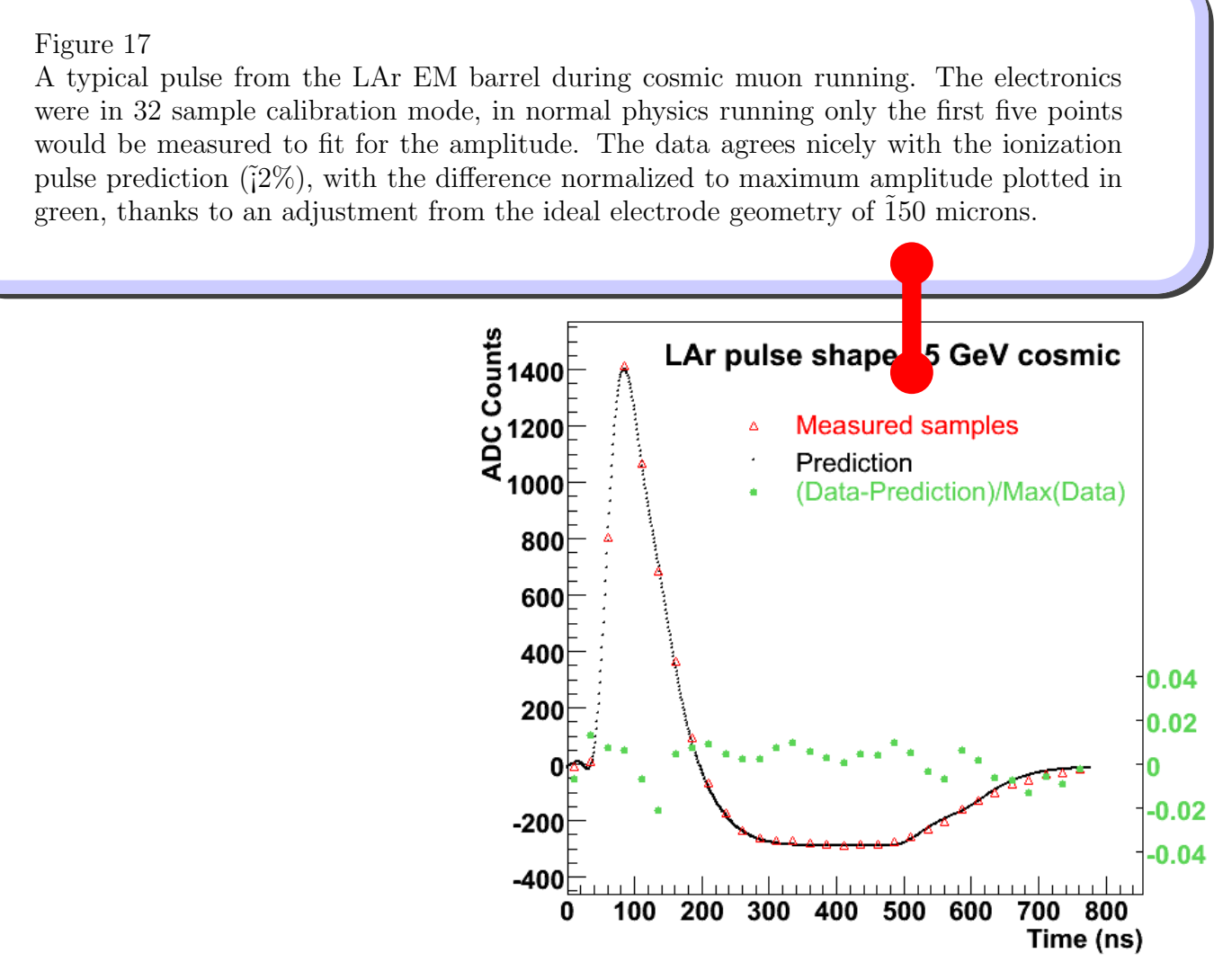


Figure 17
A typical pulse from the LAr EM barrel during cosmic muon running. The electronics were in 32 sample calibration mode, in normal physics running only the first five points would be measured to fit for the amplitude. The data agrees nicely with the initialization pulse prediction (2%), with the difference normalized to maximum amplitude plotted in green, thanks to an adjustment from the ideal electrode geometry of 150 microns.

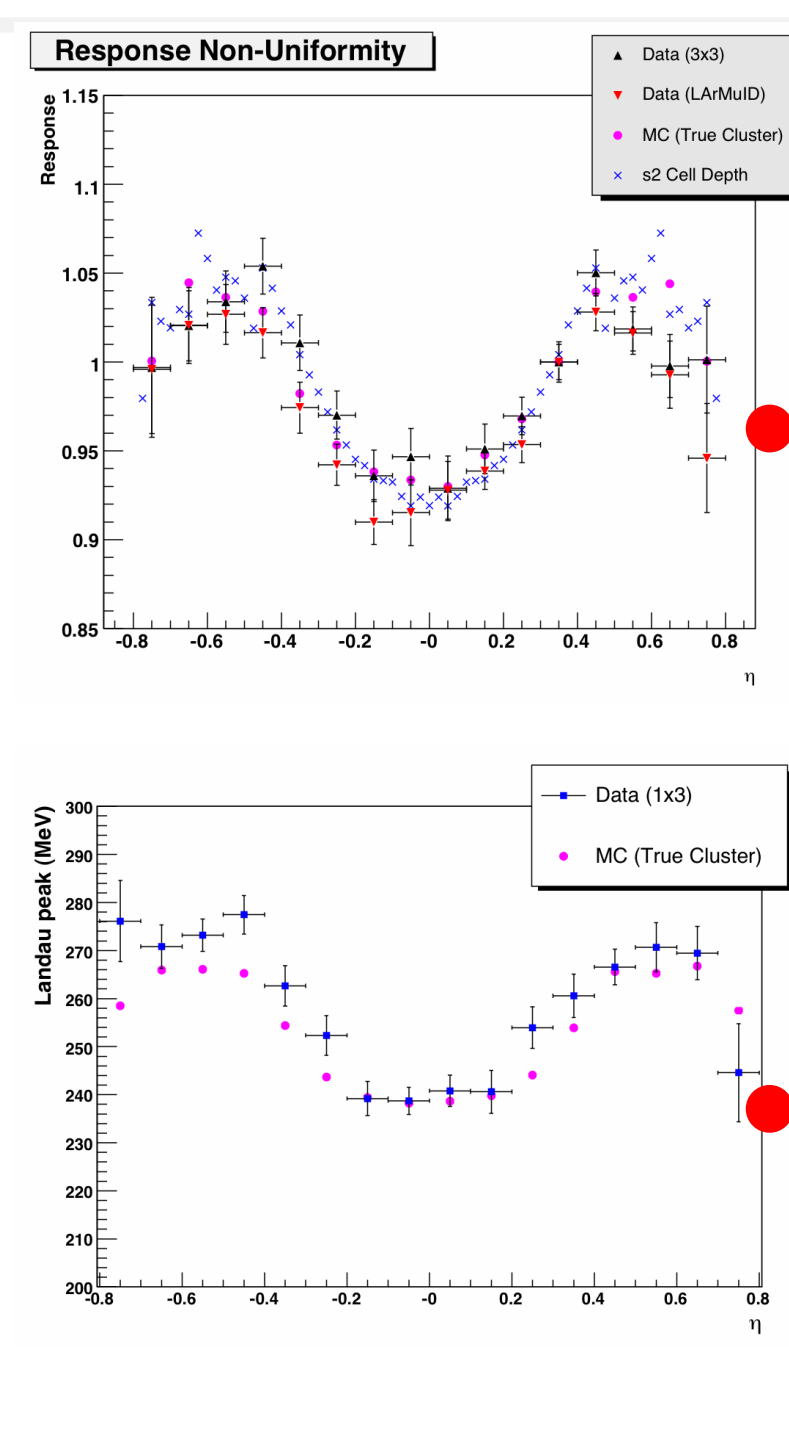


Figure 18
The Most Probable Value of energy versus pseudo-rapidity, comparing Monte Carlo to two different measurement methods of determining energy, the topological LArMud algorithm and a sliding window 3x3 cell cluster of summed energy. The y-axis is the energy normalized to a point between η = 3 or 4 and "2 Cell Depth" is the relative cell depth of the second sampling layer. The energy distribution shows the expected dependence on cell depth in uniformity to within 2% of our simulations [14].

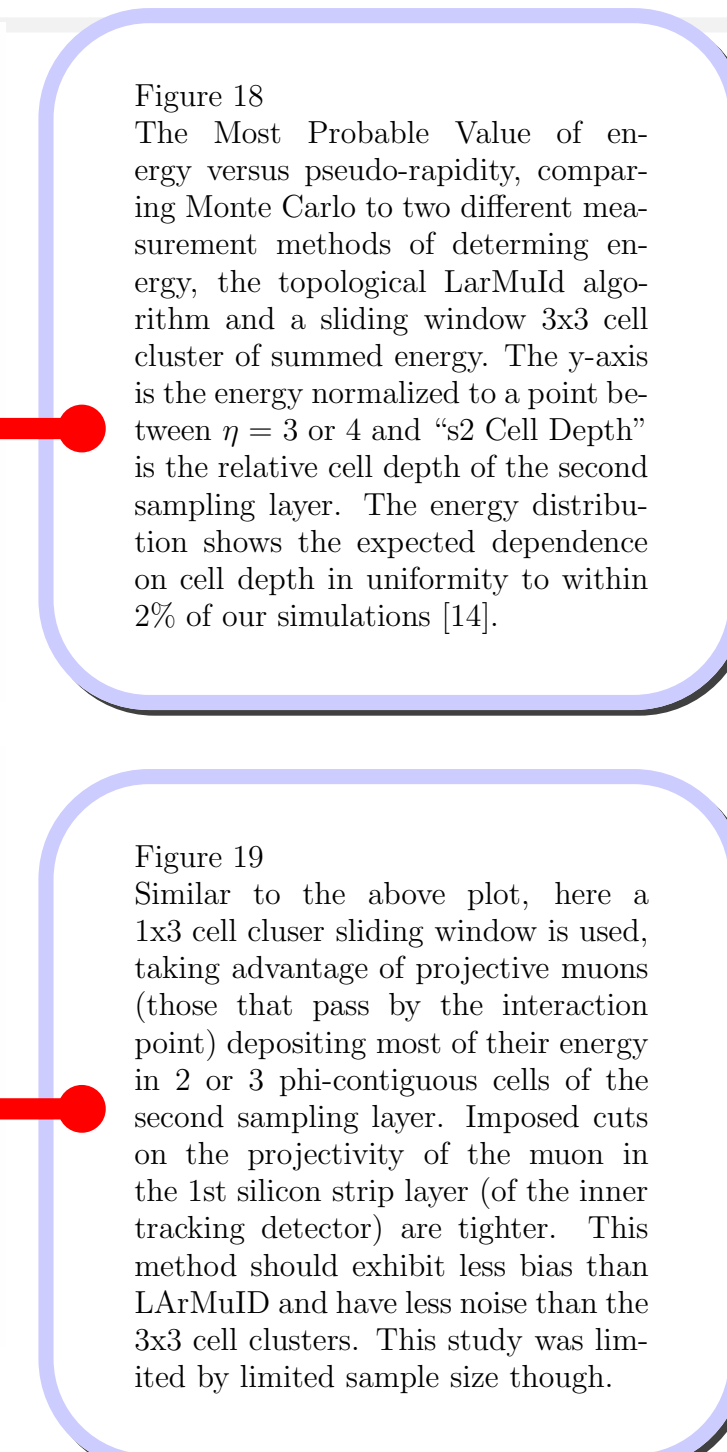


Figure 19
Similar to the above plot, here a 1x3 cell cluster sliding window is used, taking advantage of projective muons (those that pass by the interaction point) depositing most of their energy in 2 or 3 pile-up-free cells of the second sampling layer. Imposed cuts on the projectivity of the muon in the 1st silicon strip layer (of the inner tracking detector) are tighter. This method should exhibit less bias than LArMud and have less noise than the 3x3 cell clusters. This study was limited by limited sample size though.

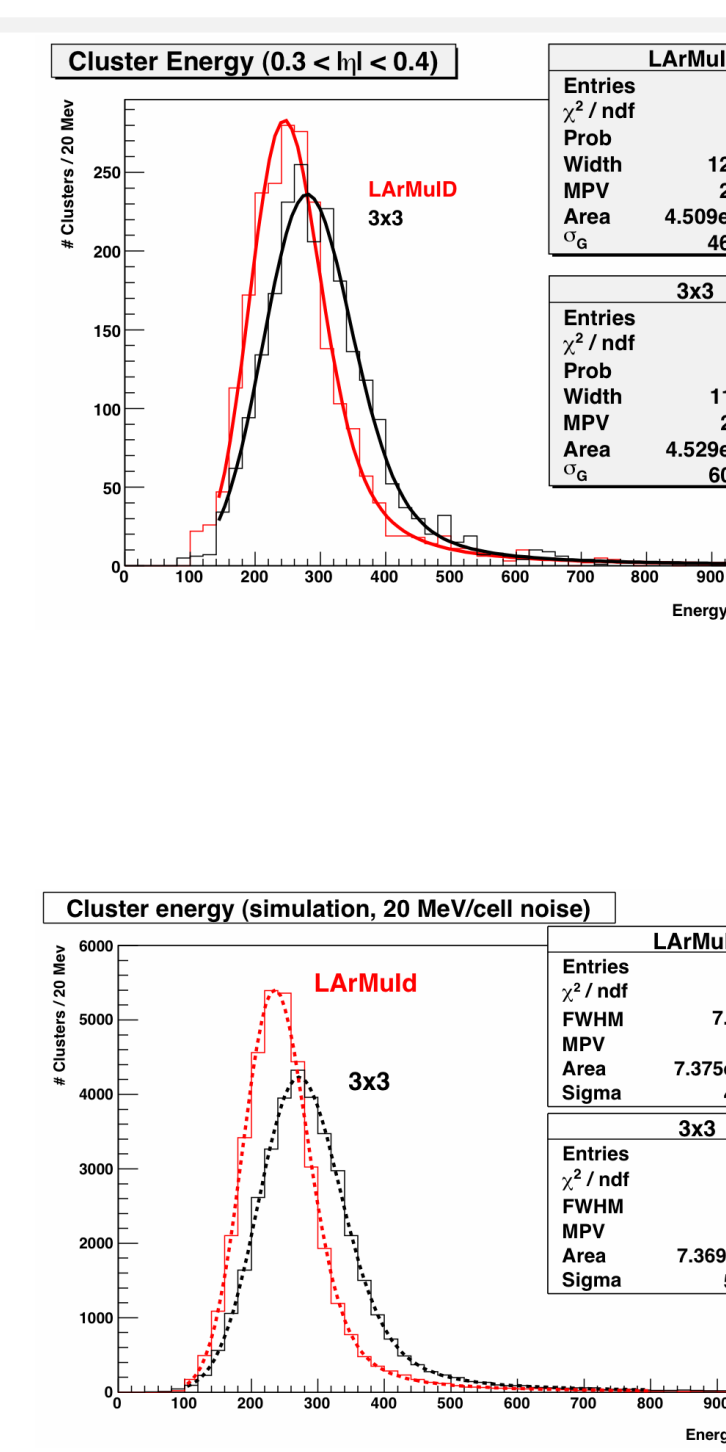


Figure 20
This plot shows the cluster energy distribution for two different cluster algorithms, both of which are restricted to cells of the second sampling layer. The clusters are taken from events which satisfy a loose projectivity requirement determined from Tile calorimeter information. The clusters shown in this figure have centers in the eta region 0.3 < η < 0.4. The LArMud algorithm is a variable size algorithm - only cells above a given threshold are added to the cluster. The 3x3 cluster is fixed in size. Both cluster energy distributions have been fit with a Landau convoluted with a Gaussian. The most probable value (MPV) of the LArMud algorithm is less than that of the 3x3 distribution as a result of a bias from only including cells with energy above a certain threshold. The 3x3 cluster is sufficiently large to capture all the relevant energy in these pseudo-projective events, and the fit Gaussian width variable is consistent with the non-correlated noise of 9 cells [14].

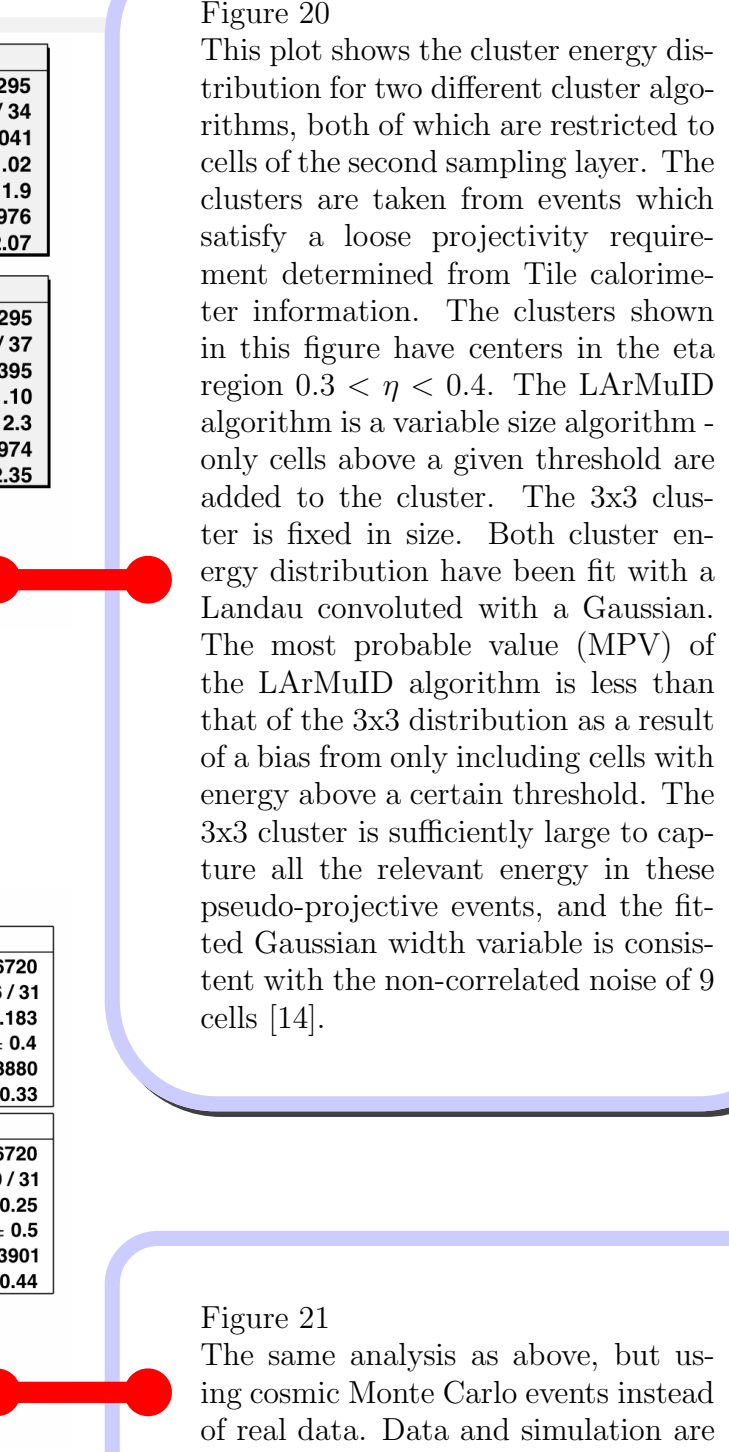


Figure 21
The same analysis as above, but using cosmic Monte Carlo events instead of real data. Data and simulation are consistent with each other.

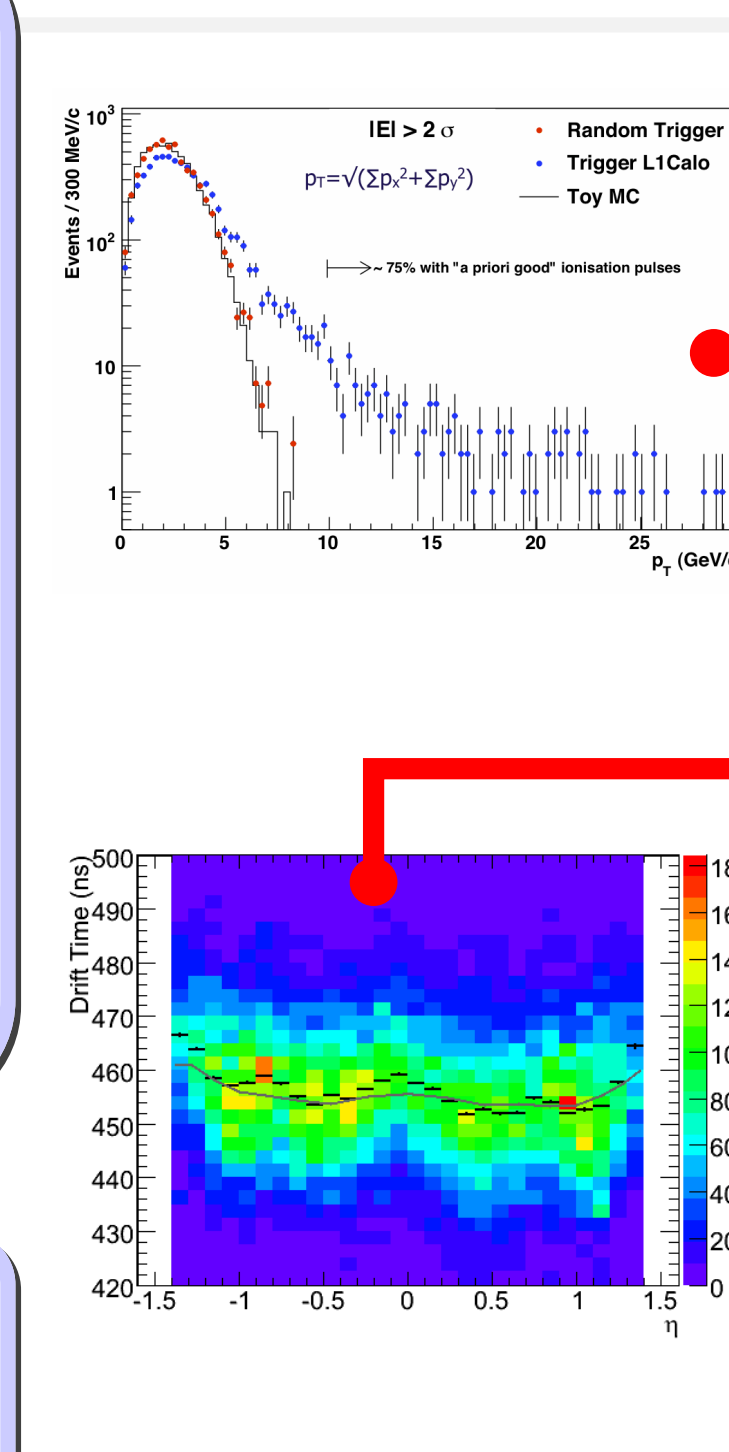


Figure 22
Attempt to examine the measurement of ΣE_T in the LAr calorimeter. ΣE_T is calculated through the scalar sum of the energy in each cell multiplied by sinθ. Only cells with energy twice the noise pedestal were used.

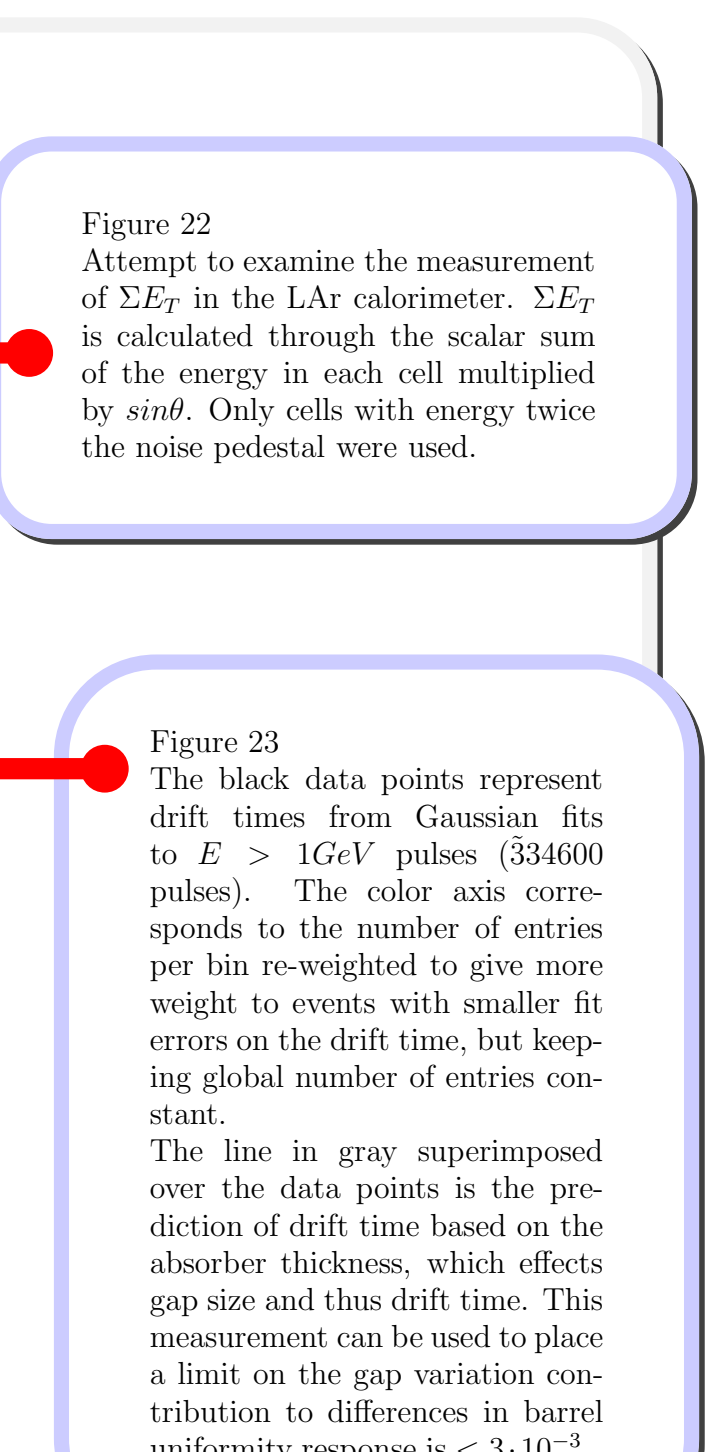


Figure 23
The black data points represent drift times from Gaussian fits to E > 1 GeV pulses (334000 pulses). The color axis corresponds to the number of entries per bin re-weighted to give more weight to events with smaller fit errors on the drift time, but keeping global number of entries constant. The line in gray superimposed over the data points is the prediction of drift time based on the absorber thickness, which effects gap size and thus drift time. This measurement can be used to place a limit on the gap variation contribution to differences in barrel uniformity response is < 3 · 10⁻⁴.

References

- [1] M. Aharrouché. The atlas liquid argon calorimeter: Construction, integration, commissioning and combined test beam results. *Nuclear Instruments and Methods in Physics Research A*, (581):373–376, 2007.
- [2] P. Krieger. The atlas liquid argon calorimeter. In *2005 IEEE Nuclear Science Symposium Conference Record*, pages 1029–1033, 2005.
- [3] B. Trovati. The atlas liquid argon calorimeter commissioning and performance from selected test beam results. In *11th Topical Seminar on Innovative Particle and Radiation Detectors*, October 2008.
- [4] K. Kopic. Liquid argon calorimeters: 2009 status and plans. Internal Talk, ATLAS Week February 2009, February 2009. Internal Presentation.
- [5] A. Bazzani et al. Atlas liquid argon calorimeter back end electronics. *Journal of Instrumentation*, 2, June 2007.
- [6] S. Simon. The liquid argon rod system. In *2nd ATLAS ROD Workshop*, October 2000.
- [7] T. Negri. Atlas tdaq system integration & commissioning. In *TIPP09*, March 2009.
- [8] H. Hadavand. Commissioning of the atlas offline software with cosmic rays. In *CHEP07*, September 2007.
- [9] A. Barrisio Poy et al. The detector control system of the atlas experiment. *Journal of Instrumentation*, 3, May 2008.
- [10] Z. Maxa. Event visualization for the atlas experiment - the technologies involved. In *CHEP 06*, February 2006.
- [11] T. Kittelman & V. Tushals. Virtual point 1 provides interactive 3d display of detector and event data. *ATLAS e-News*, July 2008.
- [12] D. Dotti et al. OHP: an online histogram presenter for the atlas experiment. In *CHEP 06*, February 2006.
- [13] A. Farbin. Atlas analysis model. In *Journal of Physics: Conference Series 119*, CHEP07, 2008.
- [14] D. Rousseau. The atlas liquid argon calorimeter: test beam, installation and commissioning. In *2007 IEEE Nuclear Science Symposium Conference Record*, November 2007.